Report on the Behaviour of ISOCAM LW Darks

P. Roman & S. Ott

ISO Data Centre, Astrophysics Division, ESA, Villafranca, Spain

Version 1.2 - June, 1999

Abstract. In this report we present the temperature dependence, data reduction and temperature correction model of the dark current of ISOCAM/LW detector.

The CAM *parallel-mode darks* of 21 revolutions, for all integration times (with the exception of 0.28 seconds) and the CAM prime *calibration darks*, longer than 30 minutes, were retrieved from the archive and processed.

As a first step, the data were dark corrected for the long and the short-term drift via the standard dark model (Biviano et al., 1998b). Then deglitching MMMS (Multi Method, Multi Step) was applied. The average value of the dark current with more than 50 good pixels per frame was determined and correlated with the detector temperature.

As first results, we found:

- The temperature dependence varies with the integration time.
- The correlation between temperature and dark current does not present any time lag.

By analysing all these data, we can build a model for the LW calibration dark, that depends on the temperature of the CAM detector and on the integration time, for the moment with the exception of 0.28 seconds. In this way the RMS value of the mean dark current decreases typically 20% with respect to the uncorrected value (with a maximum of 30%); and 10% with respect to the correction proposed by Biviano et al.

1. Introduction

In this document we describe the study and last results on the temperature effect on the dark current of ISOCAM/LW detector.

Our starting point is the work performed by Biviano et al. (1998b). It has been shown that there are three significant drifts of the LW dark-current: the first one through the ISO mission, on a timescale of days (long-term drift); the second one within each single revolution, on a time scale of hours (short-term drift); and a third one due to the dependence of the dark current on the temperature of the CAM detector. The impact of each of these effects can be summarised as follows:

- Long-term drift (~ -2 ADU from the beginning to the end of the ISO mission).
- Short-term drift (~ +/- 0.5 ADU during a revolution).
- Temperature dependence (0.5 ADU for the full range of temperature variation, few hundreths of a Kelvin).

Biviano et al. concluded that the temperature dependence is the same for all pixels and for all integration times and follows a linear relation.

In this work, we have analysed in detail the temperature dependence for each integration time in order to establish a more accurate *temperature correction model.* For this purpose we have used darks measured in the CAM parallel mode of observation. CAM parallel-mode is performed using a reduced telemetry rate when other instruments are observing in prime mode. For this observation mode, the camera was put into the dark configuration and switched into the sample mode, which produces one image around every 24 seconds. CAM parallel-mode darks are available for all the integration times with the exception of 0.28 seconds.

We have also studied a proper characterisation of a possible *time lag* between dark current and temperature. In this case we have used data provided by the *calibration darks* (darks measured during calibration-dedicated revolutions).

2. Data Reduction

The dark data reduction was performed using 2 sets of data:

- CAM parallel-mode darks of 21 revolutions, for all integration times (with the exception of 0.28 seconds).
- CAM calibration darks listed in ISOCAM Calibration Detailed List and longer than 30 minutes.

<u>*Stabilisation*</u>

A quality check is applied on each revolution in order to select only the stabilised data. Parallel-mode darks are usually close to stabilisation with the exception of images measured just after activation, hand-over and, in a few cases, after CAM prime observations. In figure 1 we can see the mean dark current for revolution 758; the peak at readout 1250 indicates hand-over and 100 frames (40 minutes) are needed until stabilisation is reached. These affected frames must be removed for the data reduction.

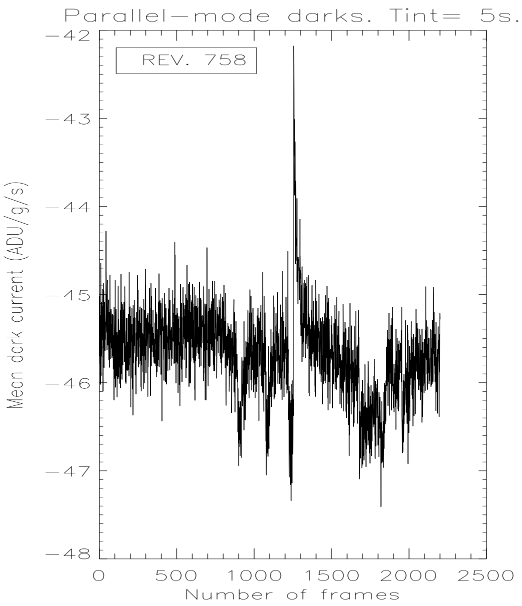

Figure 1 Mean dark current of a parallel-mode dark after standard deglitching. Note the hand-over effect around frame number 1250.

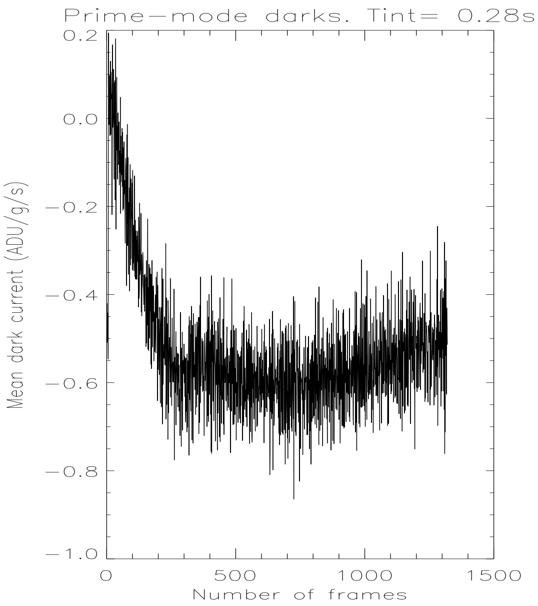

Figure 2. Mean dark current of a Calibration dark after dark correction and MMMS deglitching. Stabilisation is reached around frame number 400.

On the other hand, only a few prime calibration darks have reached stabilisation. This is due to the previous illumination conditions and the relatively long stabilisation time of the detector. However, no significant variations in the detector temperature occurred for these measurements, so they could not be used to determine the temperature dependency of the dark. Figure 2 shows the mean dark current of a calibration dark after standard dark correction and MMMS deglitching; the previous illumination effect is visible until frame number 400.

Dark correction

The data were dark corrected via the standard dark correction model, see Biviano et al. for a complete description. The model was used to correct the following two effects:

- The long-term drift: a linear decrease of the dark current from a revolution to another.
- The short-term drift: a non-linear modification of the dark current within a single revolution.

The linear dark correction depending on the detector temperature was not applied.

In figure 3, we compare revolution 748 corrected via the time-independent library dark method (in the upper plot) with the correction using the standard dark model (lower plot). The short-term drift (downwards) apparent in the upper plot is no longer visible in the lower one. Also remarkable is the global offset, induced by the long-term drift, obtained with the time-independent library dark method. For this example, data were previously deglitched with the MM method (Multiresolution Median), Starck et al., 1998

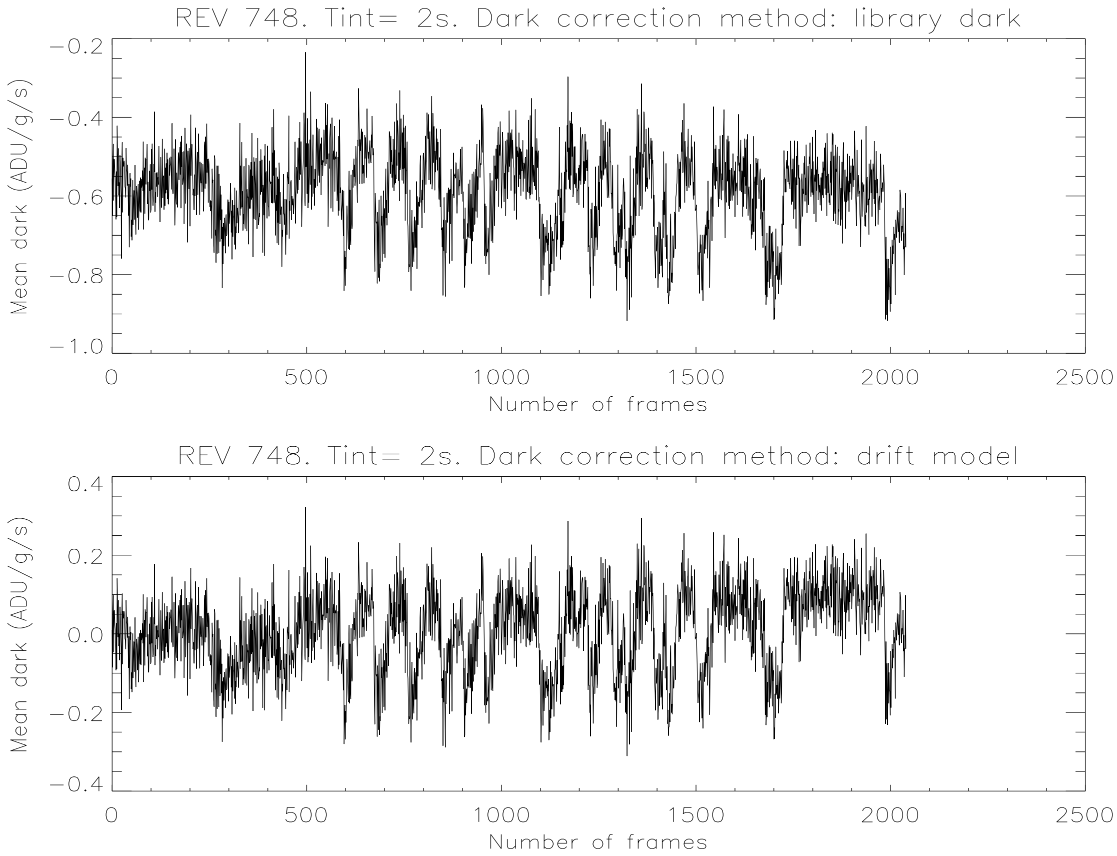

Figure 3. Mean dark current using two methods: time-independent library dark method (upper plot) and standard dark correction (lower plot). Note the global offset in upper plot

Deglitching

Different deglitching methods have been tested in the data reduction. After a comparison, MMMS was selected as the most appropriate in the analysis of the temperature dependence. In terms of correlation of the dark current with the temperature, see fig. 4, no significant differences are found by using different deglitching methods. However, MMMS provides a lower RMS level of the mean dark current than the other tested deglitching methods. In figure 5, we show the mean dark current calculated for each temperature range with the RMS error bars for MMMS, MM and TEMP deglitchers.

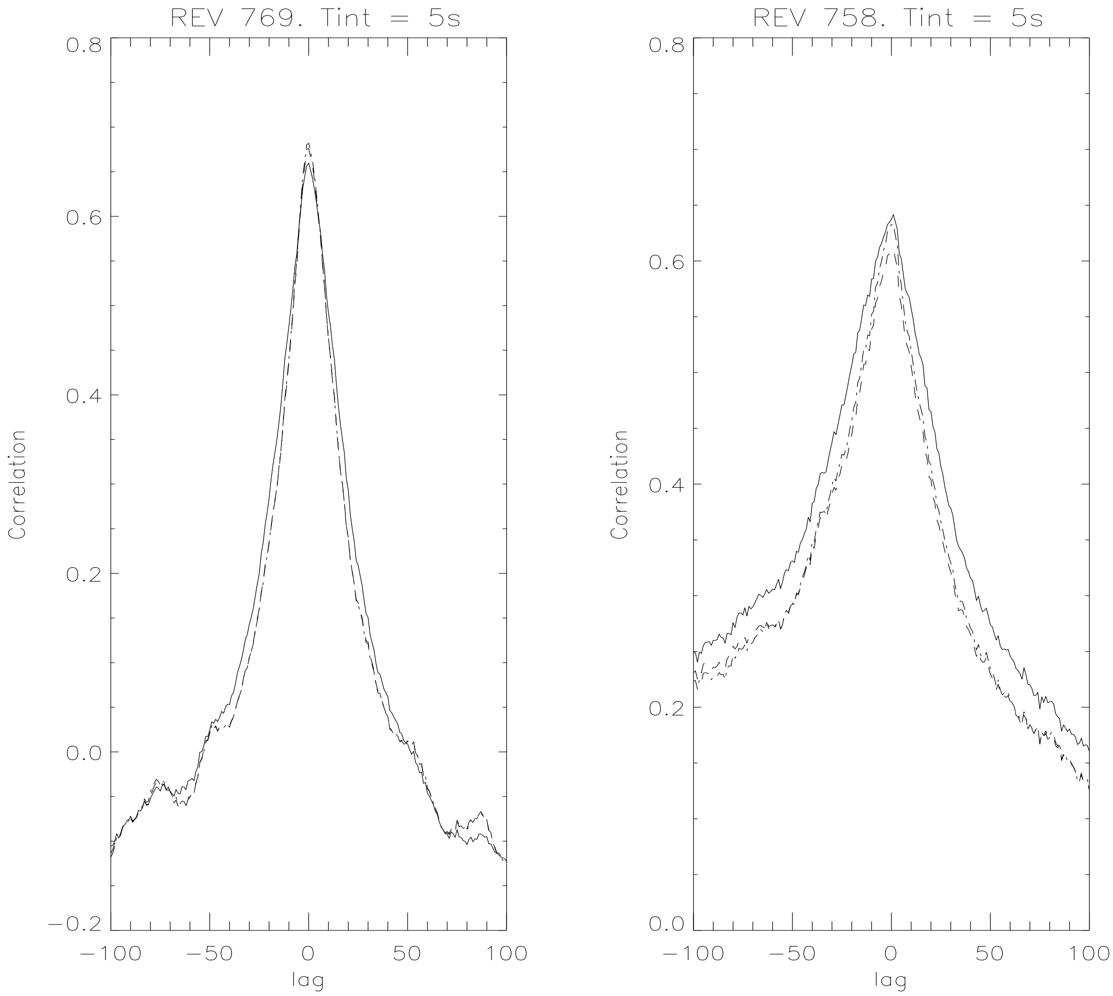

Figure 4. Correlation of the mean dark current with the temperature for three different deglitching methods: MMMS, MM and TEMP, (solid, dashed, and dot dashed line, respectively) for two revolutions.

Deglitched MMMS is applied in three steps:

- MM deglitching (nscale = 6, nsigma = 4), to eliminate strong glitches.
- TEMP deglitching with 2 sigma clipping to reject glitches undetected by MM.
- Second run of the above steps.

After comparing different sequences to perform the data reduction, we have first applied the standard dark correction and second the deglitching. This sequence yields a better result in the deglitching and in consequence, the RMS of the mean dark current decreases ~ 7%.

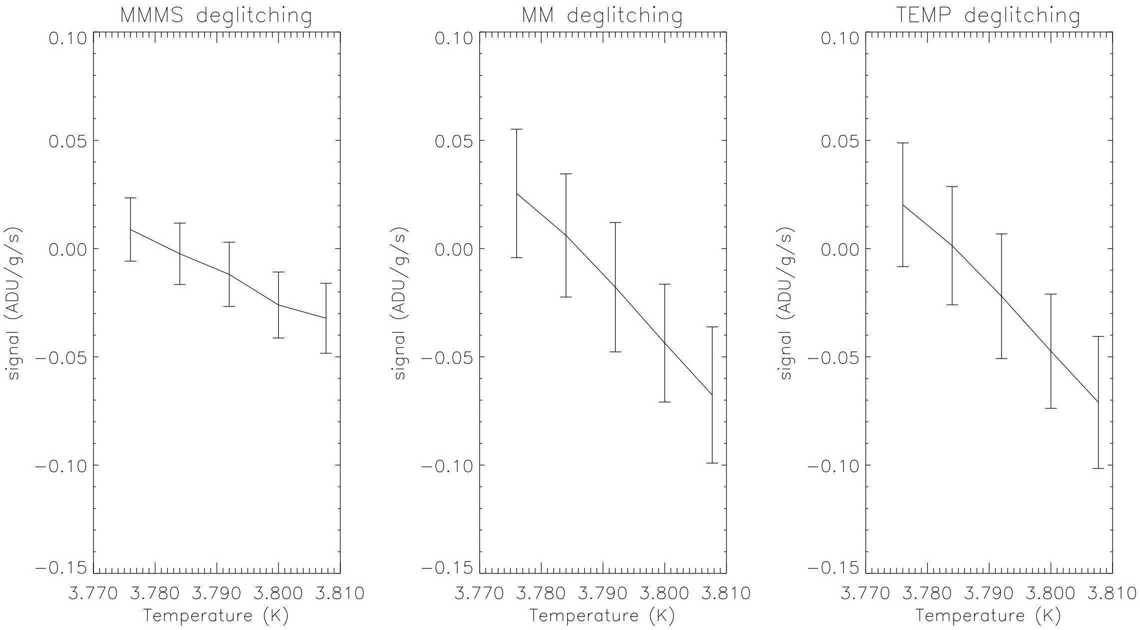

Figure 5. Average of the mean dark current with standard dark correction vs. the different temperature ranges: after MMMS deglitching (left-hand panel), after MM deglitching (middle panel) and after TEMP deglitching (right-hand panel). Note the lower error bars for MMMS deglitcher.

3. Temperature Dependence

The mean dark value of readouts containing more than 50 good pixels was determined and correlated with the detector temperature.

The CAM detector temperature ranges from 3.76 to 3.82 K. Typical values are 3.776 and 3.784. In figure 6 we plot the distribution of the mean dark current vs. the temperature for revolution 818 (Tint = 10s).

We have clearly stated the existence of a relationship between the mean dark current and the detector temperature. Whenever the temperature increases, the dark current decreases and viceversa. This effect is shown in figure 7, where we plot the mean dark current (after changing its sign, for clarity) and the temperature for two different revolutions and integration times.

The noise signal in the dark current is due to the addition of three different contributions:

- Readout noise. It should be constant for all the integration times.
- Noise induced by glitches.
- Noise induced in the dark current process.

The second contribution factor increases with the integration time; the same is expected (but difficult to confirm) for the third one.

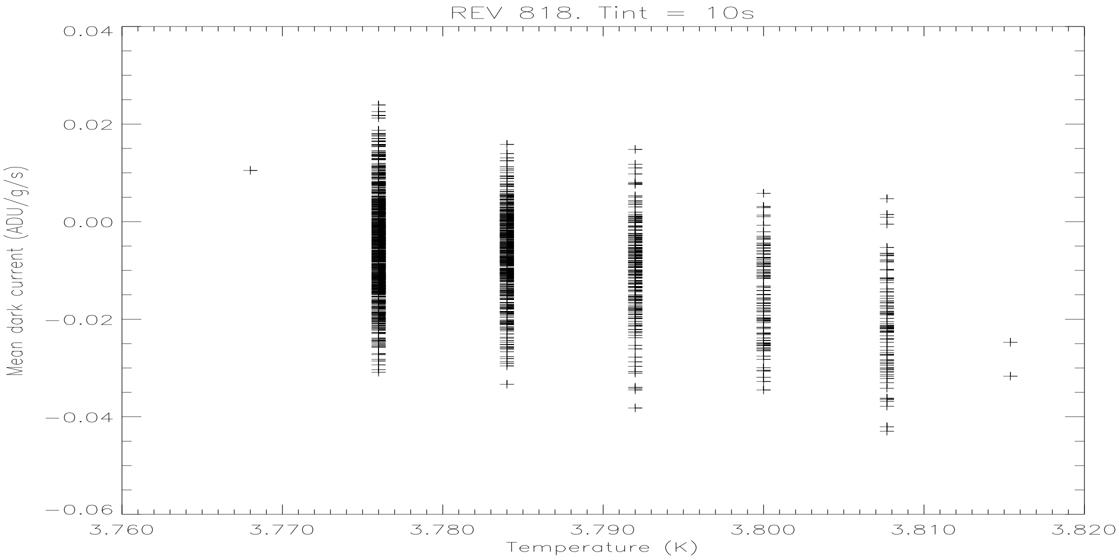

Figure 6. Distribution of the mean dark current vs. the temperature for revolution 818 (Tint = 10s).

Experimentally, we have observed that the noise (measured in ADU) increases with the integration time; in table I we can see the mean RMS noise value in ADU of 12 revolutions (3 per each Tint.) after standard dark correction and MMMS deglitching. The RMS was determined selecting readouts without temperature variations and (when possible) using the first part of the revolution to avoid time-drift effects.

Table I. Mean RMS noise in ADU of 12 revolutions (3 per each Tint.) after standard dark correction and MMMS deglitching.

	Tint = 2s	**Tint = 5s**	**Tint = 10s**	**Tint = 20s**
rms (ADU)	0.11	0.12	0.14	0.17

Table II. Correlation factors of the mean dark current with the temperature for 20 revolutions and for the available integration times.

Tint = 2 s	**Tint = 5 s**	**Tint = 10s**	**Tint = 20s**
0.55	0.70	0.65	0.28
0.57	0.76	0.55	0.36
0.55	0.70	0.55	0.42
0.72	0.64	0.39	0.55
0.72	0.65	0.48	
	0.72		

Table II shows the maximum correlation of the mean dark current with the temperature calculated for each revolution and for all integration times (with the exception of 0.28).

The correlation between dark current and temperature is highly affected by the noise level of the dark current. As the noise increases with the integration time, we observe (in general) a decrease in the correlation factor. In figure 8 we can see the correlation of the mean dark current with the temperature for a representative revolution of each integration time. But even considering a determined integration time, we obtain different results. The *quality* of the correlation improves with two factors:

- The number of temperature excursions.
- The temperature range of the temperature excursions.

These factors should be taken into account for performing a data selection in a future work.

Establishing the relation between dark current and temperature is hampered by the poor temperature discretization of the detector (we have found only seven values). This poor discretization might well be the limiting factor to reach a "perfect" temperature dark correction.

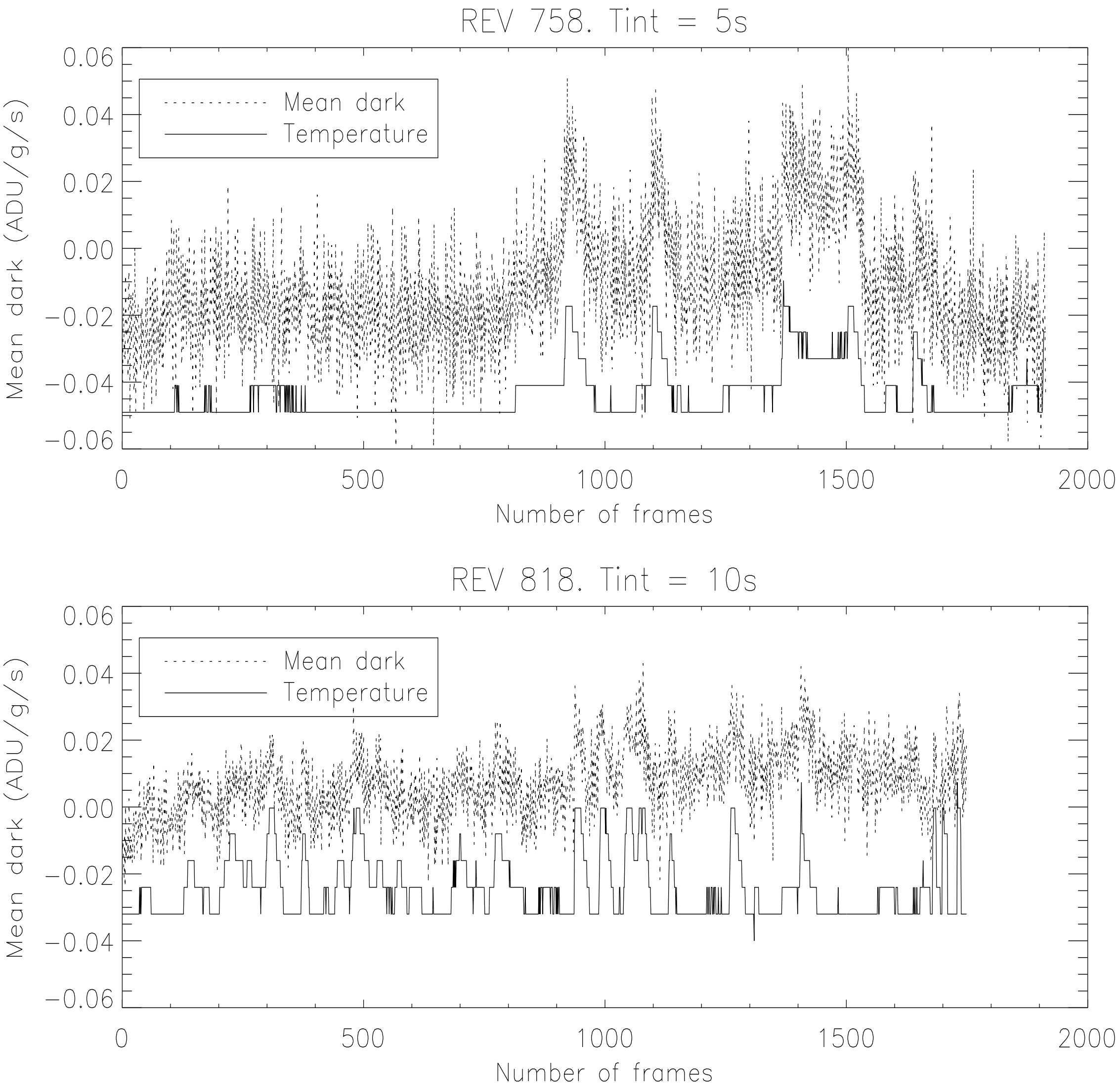

Figure 7. Mean dark current (after changing its sign, for clarity) and Temperature.

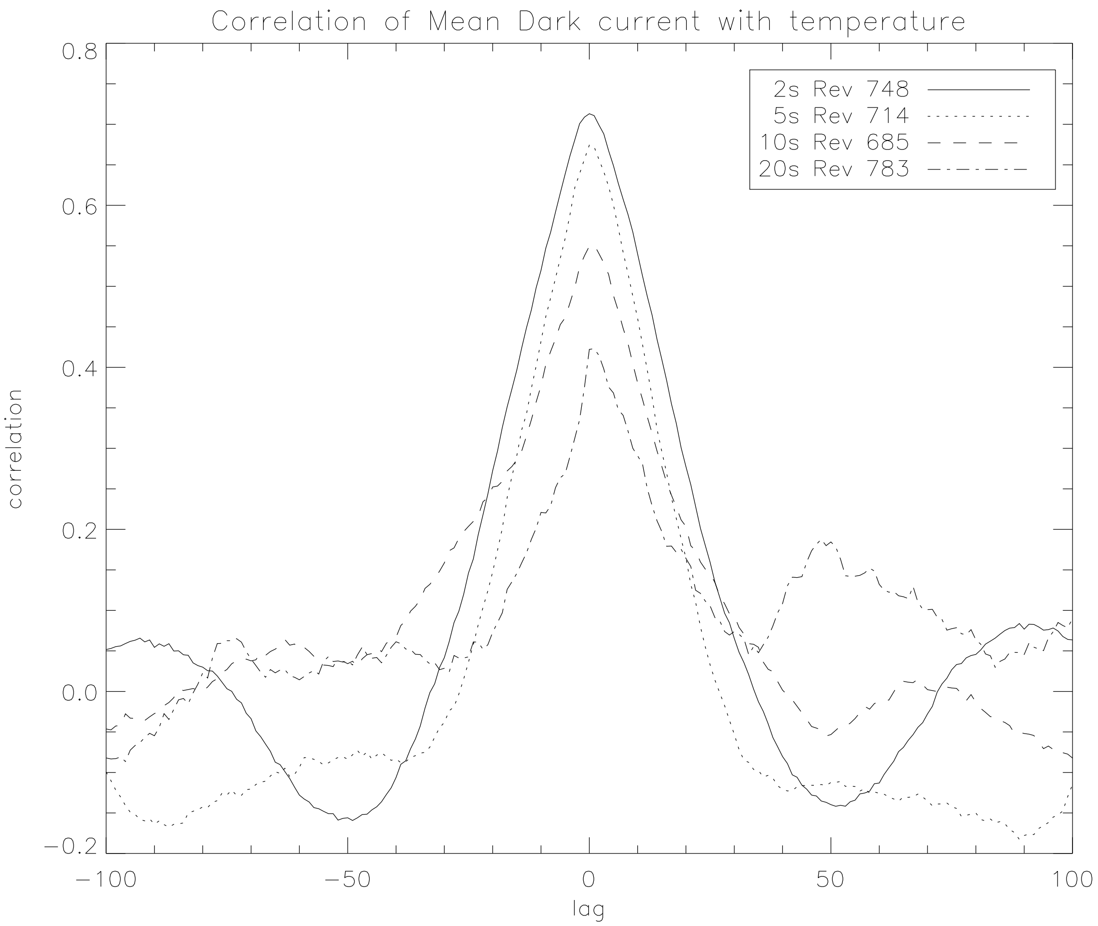

Figure 8. Comparison of correlations for different integration times

4. Temperature Correction

Our goal before establishing a temperature correction model is to analyse if the temperature dependence of the dark current presents a different behaviour with the integration time.

We have worked with four data sets. Each set contains the mean dark currents of all revolutions available per integration time (2, 5, 10, 20s). As we explained in section 2, data were stabilised, dark corrected (using the standard dark model) and deglitched (with MMMS method). On each data set we have performed the following steps,

<u>*Per revolution:*</u>

- Data distribution on the different temperatures values**:**

  $\mathbf{T_1} =$ < 3.76800 K
  $\mathbf{T_2}$ = 3.77600 K
  $\mathbf{T_3}$ = 3.78400 K
  $\mathbf{T_4}$ = 3.79200 K
  $\mathbf{T_5}$ = 3.80000 K
  $\mathbf{T_6}$ = 3.80769 K
  $\mathbf{T_7} =$ > 3.81538 K
- Evaluation of st*atistical parameters: mean, rms and uncertainty of the mean.*

Per integration time:

- Shift of all the revolutions to a reference value. The long-term drift correction applied with the standard dark model is not perfect leading to a revolution dependent offset. To compensate this offset a slight shift is introduced.
- Distribution of all darks (merging all revolutions) according to the temperature values.
- Evaluation of st*atistical parameters: mean, rms and uncertainty of the mean.*

Around 70% of the data are concentrated between 3.776 and 3.784 K. In table III we can see the percentage of readouts distributed in the different temperature values.

Plotting the histograms of one data set per each temperature value, we can observe that our data follow a Gaussian distribution. Figure 9 shows the histogram for all revolutions at 2s (upper left-hand panel) and the histograms of the same data set as a function of the temperature. We have not included the extreme temperatures, T1 and T7, because of the low number of data available. It is also here evident that the most of the data are located around T2 and T3, upper middle and right-hand panel.

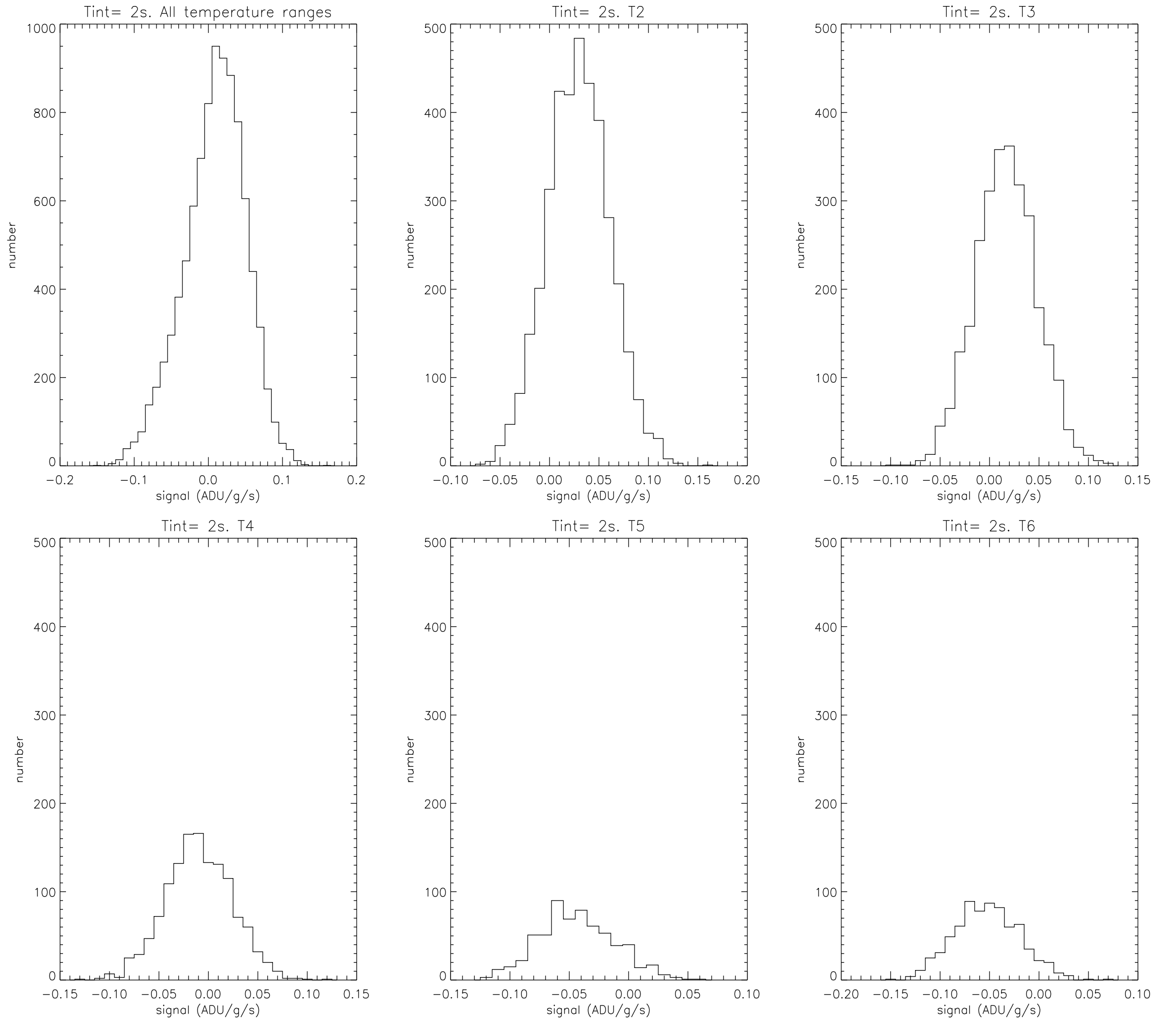

Figure 9. Histogram for all revolutions at Tint = 2s (upper left-hand panel) and histograms of the same data set as a function of the temperature. Most of data are located around T2 and T3 (3.776 to 3.784 K).

Table III. Number of readouts (in percentage) distributed in the different temperature values. Note that ~ 70% of the data are distributed between two temperatures, T2 and T3 (3.776 to 3.784 K)

T	Tint = 2 s	Tint = 5 s	Tint = 10 s	Tint = 20 s
T1	0.15	0.1	0.01	0.01
T2	40.4	58.4	48.9	49.5
T3	30.4	18.8	25.9	22.1
T4	14.4	8.1	10.3	13.8
T5	6.7	7.3	7.9	9.3
T6	7.9	7.3	7.0	5.3
T7	0.05	0.01	0.01	0.01
Number of readouts	9259	11653	7981	2964

The average value of the mean dark current vs. temperature of all reduced revolutions for each integration time is shown in figure 10. The error bars correspond to the *uncertainty in the mean* (standard deviation divided by the square root of the number of samples). As we have mentioned in the previous paragraph, we have excluded the data corresponding to the extreme temperatures as there are very few points at these temperatures. For illustration purposes, all the revolutions have been shifted to zero at the temperature value of 3.776 K.

As it can be observed, each integration time seems to have a different behaviour for the dependence of the dark current with the temperature. In general, the slope of the curve decreases when the integration time increases.

If the temperature changes in a scale of time lower than the integration time, the dark current dependence on the temperature will be masked because the current variations are integrated during the integration time. The consequence of this effect, together with a higher RMS noise for long integration times, can be appreciated in a higher data dispersion for long integration times (10 and 20s), see lower panels of figure 10.

As the applied standard dark correction, for the short-term drift, is not always perfect, we observe for most of cases a linear downward trend over the mean in the last part of the revolution, see figure 11. This fact, together with the signal noise, could explain the differences found between revolutions for the same integration time.

5. Time lag (prime darks)

As prime darks provides a better time resolution than parallel darks, the former can be used to verify the time-coincidence between detector temperature and dark level.

Only few prime dark measurements for 0.28, 2, 5 and 10 seconds of integration time have reached a stable value. The data available for 20 seconds are not stabilised.

To study a possible time-lag, we have focused our interest on 0.28 prime darks, because this integration time provides the maximum time resolution (one second).

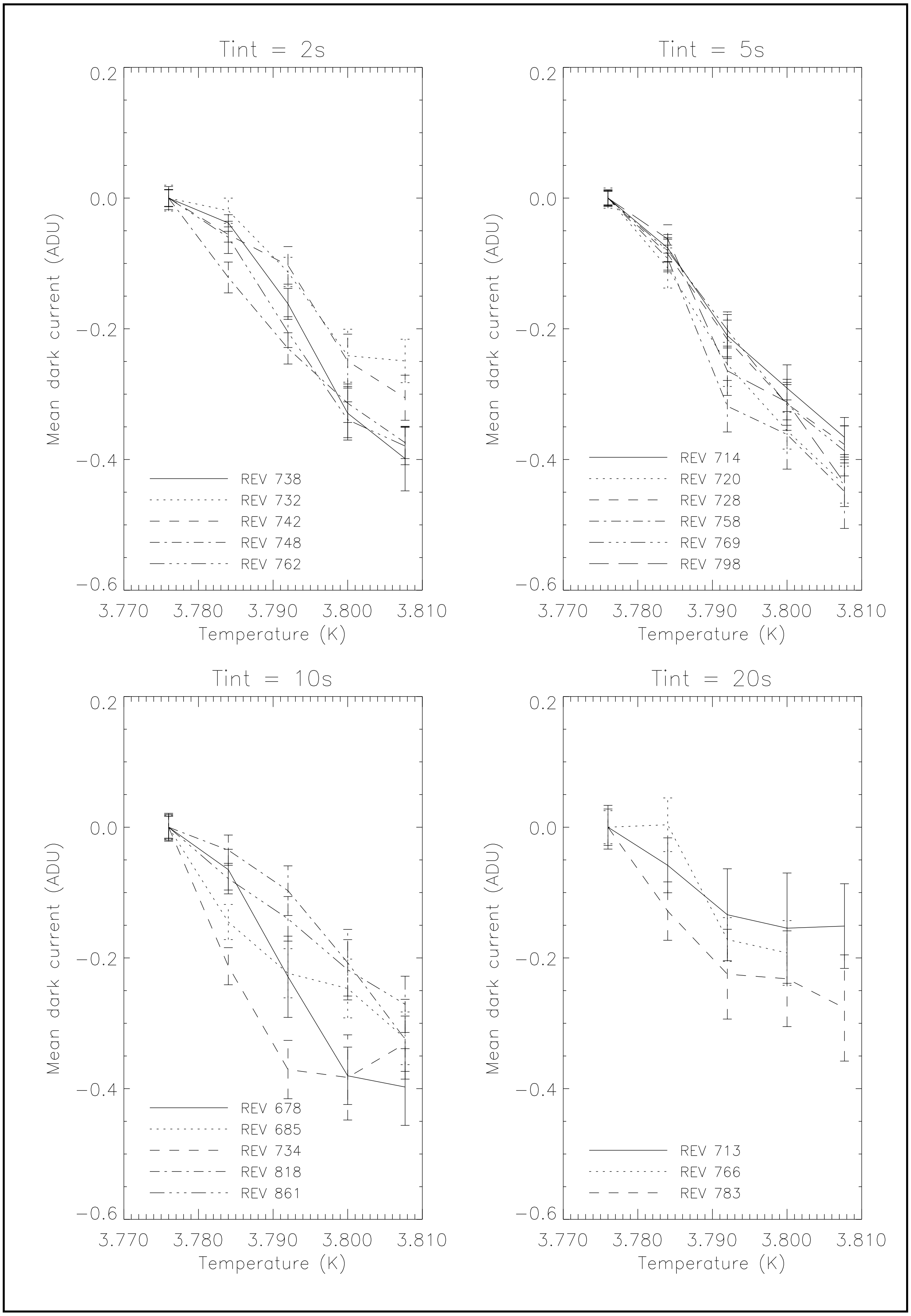

Figure 10. Average value of the mean dark current vs. temperature of all reduced revolutions for each integration time. The error bars correspond to the uncertainty in the mean considering 3 sigma.

In figure 12, left-hand panel, we can see the mean dark current for a prime dark measurement at 0.28 seconds of integration time overplotted with the temperature. In right-hand panel we show the correlation with the temperature. As expected, the maximum correlation is obtained when there is not any lag between both signals. Therefore we can assess that the time lag (if any) is shorter than 0.5 seconds.

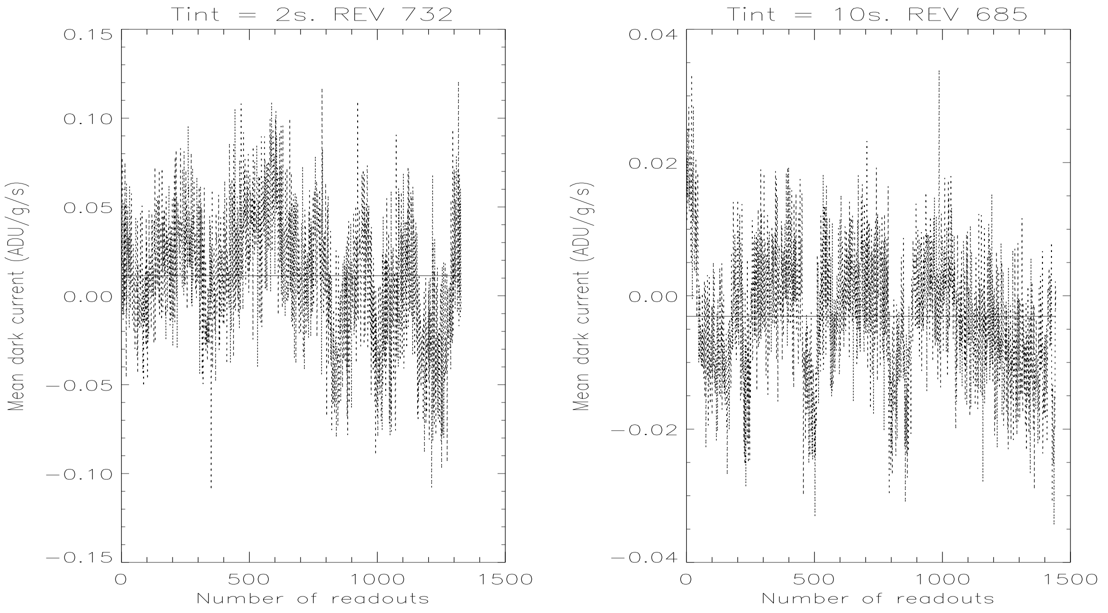

Figure 11. Mean dark current (dashed line) after standard dark correction. The solid line indicates the mean value. Note the downward trend to the end of the revolution.

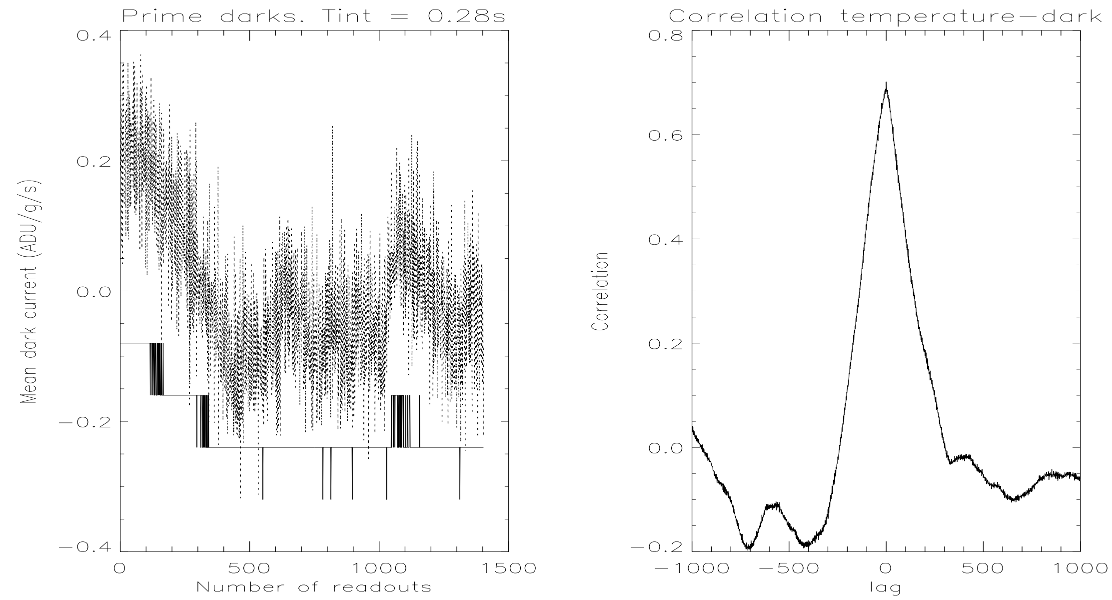

Figure 12. Left-hand panel: mean dark current for a Prime dark measurement at 0.28 seconds of integration time (dashed line) and the overplotted temperature (solid line). Right-hand panel: correlation with the temperature. As it was expected, the maximum correlation is obtained when there is not any lag between current and temperature.

6. Temperature Correction Model

From the results described in paragraph 4, it was decided to create a correction model for each integration time, namely 2, 5, 10, 20 s. The model was calculated using the average values of the mean darks for each temperature and for each integration time. It presents two main characteristics:

- It depends on each temperature.
- It is different for each integration time.

The temperature correction model can be described by the following relation,

$$DARK_C = DARK_O - F(T)$$

where $DARK_C$ and $DARK_O$ are the temperature corrected and observed values, respectively, of the dark current in ADU/g/s and F is the temperature dependent correction factor. The correction factor values are provided in annex 1 at the end of this document.

In figure 13, we can see the four integration time dependent temperature models and the temperature correction established by Biviano et al., hereafter referred as Biv/Sau model. Note the slope changes for the different temperature values. In comparison with Biv/Sau model, the slope differences are more evident between 3.776 and 3.784 K where the 70% of the data are concentrated.

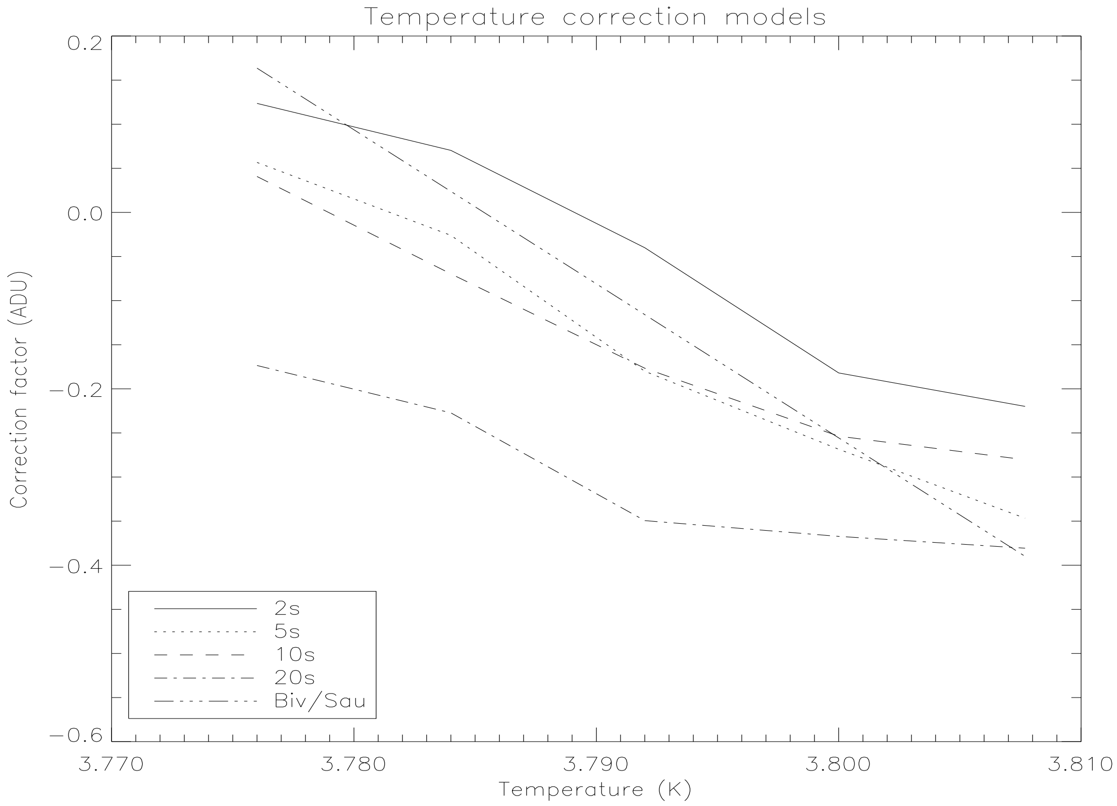

Figure 13. Integration time dependent temperature models and temperature correction established by Biviano et al. (Biv/Sau). Note slope changes with the different temperature values for the new temperature models.

6. Results

In figure 14 we provide an example of a temperature correction using Biv/Sau model and the new proposed model. In the upper panel we show the mean dark current for revolution 685 (after changing its sign, for clarity) and the temperature; the signal was dark corrected and deglitched. In the middle and lower panel we see the same revolution after applying Biv/Sau and new temperature correction, respectively. In general we have checked that after applying the new model, the RMS noise value of the mean dark current decreases typically a 20% with respect to the uncorrected value; and 10% with respect to the Biv/Sau correction.

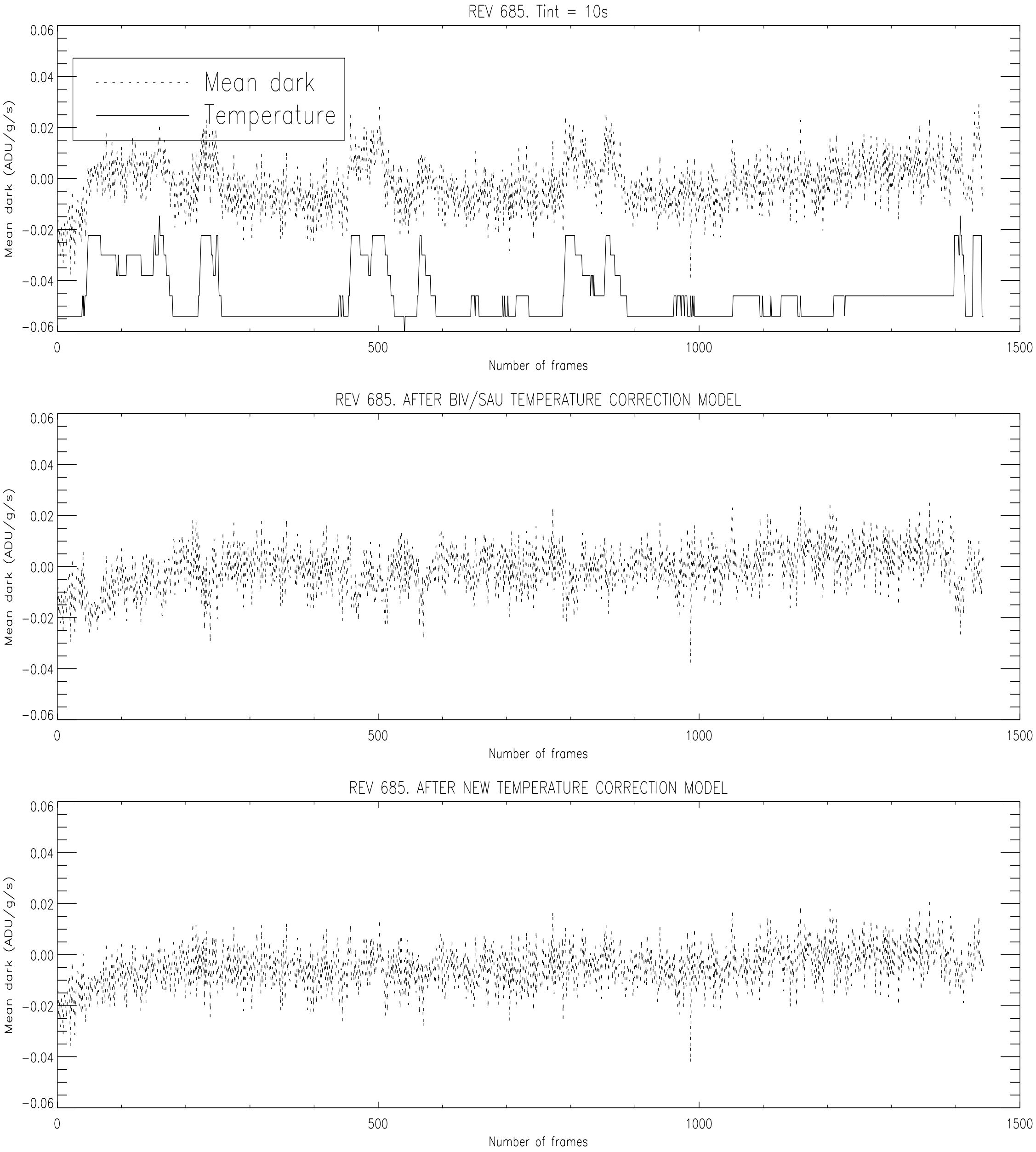

Figure 14. Mean dark current and temperature of revolution 685 before (upper panel) and after temperature correction using Biv/Sau model (middle panel) and the new proposed temperature correction model (lower panel).

To compare the new model with Biv/Sau model, we have applied the *reduced Chi-square* test to all the reduced revolutions:

$$\chi_\nu^2 = \frac{\sum \frac{1}{\sigma_{i(model)}^2} \left[y_{i(uncorrected)} - y_{i(model)}\right]^2}{N - n - 1}$$

χ_ν^2 : reduced chi-square
σ_i : standard deviation of the model
$y_{i(uncorrected)}$: set of uncorrected data
$y_{i(model)}$: model data
N : number of data
n : number of model coefficients

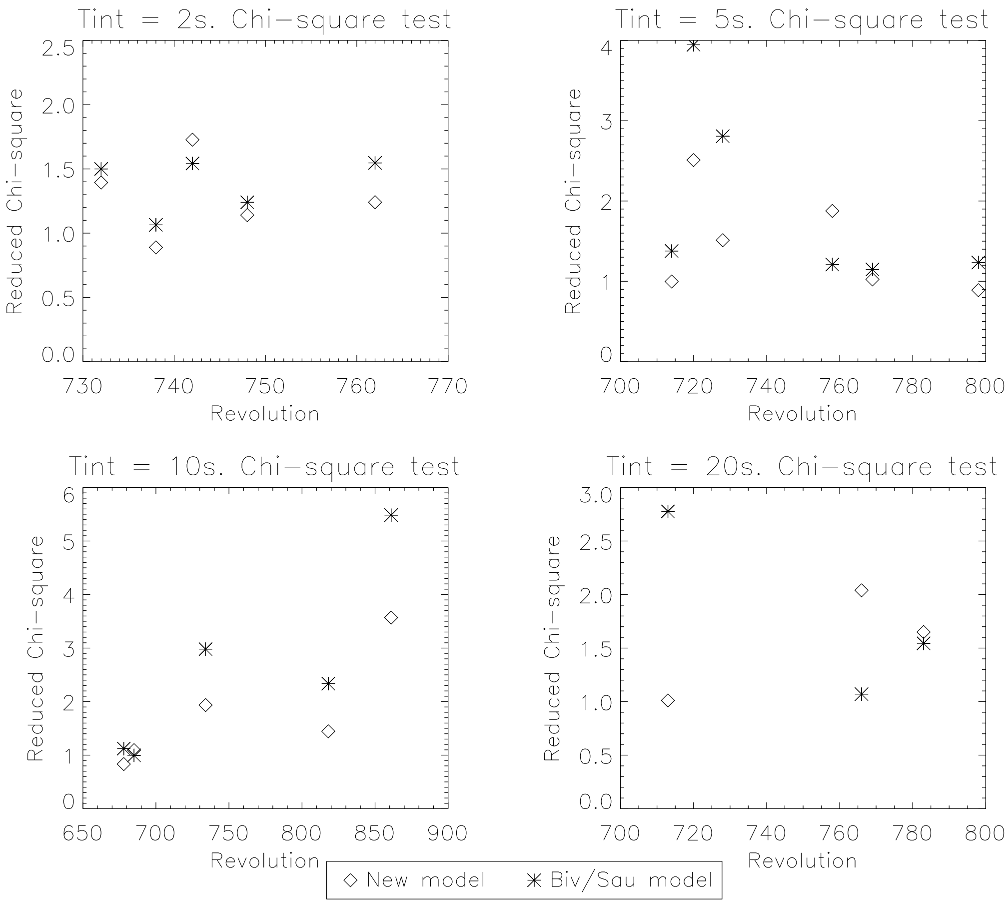

Figure 15. Chi-square test on all reduced revolutions for comparison of Biv/Sau model and new model. In most of the revolutions a better result is achieved with the new model

The results are shown in figure 15. If the fitting function (model) is a good approximation of the mean dark current (before applying temperature correction), the value of the *reduced chi-square* should be approximately unity. If the fitting function is not appropriate for describing the data, the deviations will be larger, yielding a value of *reduced chi-square* greater than one. A value of *reduced chi-square* less than 1 is a consequence of the fact that there exists an uncertainty in the determination of chi-square. As we can observe from the figure, in most of the revolutions, the values of *reduced chi-square* closer to the unity correspond to the new model correction. It is also evident that better results are achieved for short integration times (2s) and that the dispersion in the results increases with the integration time.

7. Future work

As future work we propose:

- Investigation of reached short and long-term drift quality and, if necessary, a new derivation of short and long-term drift correction parameters.
- Extension to 0.28 seconds of integration time.
- Improvement of the temperature correction model by performing a proper data selection.
- Study on how glitches affect the dark base-line level.
- Study on how space weather affects the dark current.
- Use of further improved deglitching methods.

Acknowledgements

The authors would like to acknowledge fruitful discussions with A. Pollock, A. Biviano, B. Altieri, L. Metcalfe and M. Sauvage.

References

- Biviano A. et al. 1998b, "The ISOCAM/LW detector dark current behaviour".
- Delaney M. 1998, "ISOCAM Interactive Analysis User’s Manual", Version 3.0.
- ISOCAM Observer’s Manual, The ISOCAM Team, 1994.
- Ott S. June 1999, "Report on the behaviour of LW Prime Darks", Version 1.0.
- Ott S. et al., "New deglitching algorithms for ISOCAM", in preparation.
- Ott S. et al. 1997, "Design and Implementation of CIA, the ISOCAM Interactive Analysis System", ASP Conferences Series, Vol. 145.
- Roman P. 1998, "ISOCAM Calibration Detailed List".
- Siebenmorgen et al. 1999, "ISOCAM Handbook".
- Starck J-L., Murtagh F., Bijaoui, A. 1998, "Image Processing and Data Analysis: The Multiscale Approach", Cambridge University Press.
- Bevington P. 1969. "Data reduction and error analysis for the Physical Sciences". McGraw-Hill, New York.

ANNEX 1

Temperature correction model

In the following table, we provide the values in ADU/g/s of the temperature correction factors.

	Tint = 2s	Tint = 5s	Tint = 10s	Tint=20s
T<= 3.77600	0.029	0.006	0.002	-0.004
T = 3.78400	0.017	-0.003	-0.003	-0.006
T = 3.79200	-0.009	-0.018	-0.009	-0.009
T = 3.80000	-0.043	-0.027	-0.013	-0.009
T>= 3.80769	-0.052	-0.034	-0.014	-0.009

ANNEX 2

Listing of used revolutions per integration time.

Tint = 2s	Tint = 5s	Tint = 10s	Tint = 20s
732	714	678	713
738	720	685	766
742	728	734	783
748	758	818	
762	769	861	
	798		